Pulmonary targeting microparticulate camptothecin delivery system: anti-cancer evaluation in a rat orthotopic lung cancer model

Piyun Chao[a,b], **Manjeet Deshmukh**[a,c], **Hilliard L. Kutscher**[a], **Dayuan Gao**[a], **Sujata Sundara Rajan**[a], **Peidi Hu**[a,d], **Debra L. Laskin**[c,e], **Stanley Stein**[a], and **Patrick J. Sinko**[a,c,*]

[a]Department of Pharmaceutics, Ernest Mario School of Pharmacy, Rutgers, The State University of New Jersey, Piscataway, New Jersey 08854, USA

[c]UMDNJ-Rutgers CounterACT Research Center of Excellence, Rutgers, The State University of New Jersey, Piscataway, New Jersey 08854, USA

[e]Department of Pharmacology and Toxicology, Rutgers, The State University of New Jersey, Piscataway, New Jersey 08854, USA

Abstract

Large (>6 μm) rigid microparticles (MPs) become passively entrapped within the lungs following intravenous injection making them an attractive and highly efficient alternative to inhalation for pulmonary delivery. In the current studies, PEGylated 6 μm polystyrene MPs with multiple copies of the norvaline (Nva) α-amino acid prodrug of camptothecin (CPT) were prepared. Surface morphology was characterized using a scanning electron microscope (SEM). CPT was released from the CPT-Nva-MPs over 24 hours in rat plasma at 37°C. *In vivo* CPT plasma concentrations were low (~1 ng/mL or less) and constant over a period of 4 days after a single intravenous injection of CPT-Nva-MPs as compared to high but short-lived systemic exposures after an IV injection of free CPT. This suggests that sustained local CPT concentrations were achieved in the lung after administration of the MP delivery system. Anti-cancer efficacy was evaluated in an orthotopic lung cancer animal model and compared to a bolus injection of CPT. Animals receiving either free CPT (2 mg/kg) or CPT-Nva-MPs (0.22 mg/kg CPT, 100 mg/kg MPs) were found to have statistically significant smaller areas of lung cancer (P<0.05, P<0.01, respectively) than untreated animals. In addition, 40% of the animals receiving CPT-Nva-MPs were found to be free of cancer. The CPT dose using targeted MPs was ten fold lower than after IV injection of free CPT but was more effective in reducing the amount of cancerous areas. In conclusion, CPT-Nva-MPs were able to achieve effective local lung and low systemic CPT concentrations at a dose that was ten times lower than systemically administered CPT resulting in a significant improvement in anticancer efficacy in an orthotopic rat model of lung cancer.

Keywords

Lung cancer; microparticles; passive pulmonary targeting; camptothecin

Corresponding Author. Patrick J. Sinko, 160 Frelinghuysen Road, Piscataway, New Jersey 08854, (Tel) 732-445-3831 x 213; (Fax) 732-445-3134, sinko@rutgers.edu.
[b]*Current address:* Hurel Corporation, Beverly Hills, California 90211, USA.
[d]*Current address:* Incyte Corporation, Wilmington, Delaware 19880, USA.

Introduction

In the United States, lung cancer has the second highest rate of incidence after prostate and breast cancer in males and females, respectively [1, 2]. Lung/bronchus cancer is the leading cause of death in men and women among all types of cancer. Cancer therapy is often limited by patient intolerance due to systemic side effects and high toxicities of the administered medications. Therefore, targeting potent anti-cancer drugs directly to the tumor site in the lung should result in high local drug concentrations, reduced systemic drug concentrations and a reduction in drug-induced damage to noncancerous organs. In addition, higher localized drug concentration also helps to prevent the development of multidrug resistance in cancer cells [3, 4]. Furthermore, it is also known that tumors employ angiogenesis to facilitate the nutrition required for the tumor growth [5]. Therefore, the drug-carrier described in this study may tend to concentrate in the capillary-rich cancerous sites other than the healthy parts of the lungs.

Although there are numerous new approaches such as angiogenesis inhibitors, matrix metalloproteinases inhibitors, targeting epidermal growth factor receptor (EGFR) pathways, gene therapy, and antisense therapy for the treatment of lung cancer, there has been limited improvement in patient survival rates[6]. EGFR tyrosine kinase inhibitors have been evaluated with concurrent chemotherapy in a series of phase III trials and no benefit was reported by adding either erlotinib or gefitinib to standard first-line platin-based chemotherapy in advanced non-small cell lung cancer (NSCLC) [7–10]. Bevacizumab, a FDA approved monoclonal antibody against VEGFR, which acts as an angiogenesis inhibitor for NSCLC, only offered a modest survival benefit in a limited patient population [11]. Therefore tailoring targeted therapies remains important in NSCLC treatment. Some other approaches use targeting moieties of over-expressed receptors on the surface of cancer cells, while others have targeted apoptosis, cell cycle regulators, monoclonal antibodies, vaccination, and antineoplastons with some promising results in *in vitro* studies. However, few successes have translated to the *in vivo* situation and clinic [6]. Therefore, alternative approaches such as organ-targeting provide additional options for anti-cancer drug delivery. Lung targeting can be achieved by utilizing its unique physiological features. The lung is the only organ in the body that receives the entire venous blood output from the heart. Therefore, the lung serves as a blood filter and is able to efficiently entrap a wide variety of MPs after IV administration [12–18]. A unique property of the lung is its ability to function after exposure to particulate matter, which is unlike any other organ. Mechanistically, this occurs since the lung utilizes a small percentage of its massive vascular space during rest and recruiting unused capillaries to allow the blood to continue to flow relatively unhindered during exercise or increased arterial pressure because of blocked of capillary beds within the lung [19].

As a result of the unique physiological features of the lung, macroaggregated albumin (MAA) has been used in nuclear medicine for many years to image pulmonary blood flow [20]. These flexible MPs are of a sufficient size (10 µm) such that when injected intravenously, they cannot pass readily through the pulmonary capillary bed [21, 22]. MAA accumulates in peripheral lung tissue and is thought to be cleared by interstitial macrophages [21–24] or fragmentation because of the bombardment of red blood cells [25].

It has also been shown that radiolabeled MAA MPs collect in the pulmonary capillary bed at a rate that is proportional to the blood flow [26]. Recently, our lab systematically studied the relationship between rigid MP size and lung targeting efficiency, intra-lung distribution and retention time [12]. Complete entrapment and retention of 10 µm MPs was observed for the one-week duration of the study whereas 2 µm and 3 µm MPs readily passed through the lung. A large portion (>80%) of the 6 µm MPs were retained for the first two days with 15%

being slowly cleared over the next 5 days suggesting a possible threshold size for rigid MPs. Wide distribution of 6 and 10 μm MPs throughout lung tissue provided evidence of entrapment in pulmonary capillaries but not arterioles [12].

The transient but efficient targeting of pulmonary capillaries by rigid 6 μm MPs, which was observed in our previous work, suggested that systemic administration of MPs may be an efficient alternative to inhalation for delivery to the lungs. Therefore, the objective of the current studies was to develop, characterize and assess the feasibility of utilizing a passive pulmonary targeting drug delivery system for the treatment of lung cancer. Drug-containing MPs were designed to improve the efficacy of lung cancer treatment. To take advantage of the unique ability of the lung to passively entrap MPs for drug delivery, a CPT-Nva prodrug was prepared and covalently attached to ethylenediaminetetraacetic (EDTA)-coupled PEGylated 6 μm polystyrene MPs. The results of the current studies suggest that systemic administration of pulmonary-targeted MPs may be an efficient alternative to systemic drug administration for the treatment of lung cancer.

Materials and Methods

Materials

Carboxyl modified polystyrene MPs (mean diameter 6 μm) were purchased from Molecular Probes, Inc. (Carlsbad, CA). *N, N*-diamino-poly (ethyleneglycol) (DAPEG, 3.4 kDa) was obtained from Nektar Inc. (San Carlos, CA). Ethylenediaminetetraacetic (EDTA), 4-dimethylaminopyridine (DMAP), dimethyl sulfoxide (DMSO) and 1, 3-diisopropylcarbodiimide (DIPC) were purchased from Sigma-Aldrich (Atlanta, GA). Fluorescamine was obtained from Roche Diagnostics (Indianapolis, IN). For the synthesis of the CPT–Nva prodrug, CPT was purchased from Sigma-Aldrich and Boc-norvaline was purchased from EMD Biosciences (Gibbstown, NJ). Intralipid® was purchased from Sigma-Aldrich (St. Louis, MO). A human lung carcinoma cell line, A549, was purchased from American Type Culture Collection (ATCC, Manassas, VA).

Animals—Male Sprague Dawley rats weighing between 250–275 g were purchased from Hilltop Lab Animals, Inc. (Scottdale, PA). Male nude rats (200–250 g) were purchased from the National Cancer Institute at Frederick (Frederick, MD). Sprague Dawley rats were housed in standard rat cages. Nude rats were housed in sterile microisolation rat cages. Rats were fed a standard rat diet, had free access to water and were housed in a room with a 12-hour light-dark cycle for at least one week before studies. All rat studies were performed under approved protocols from the Use and Care of Animal Committee at Rutgers University in AAALAC accredited facilities.

Preparation of CPT-Nva-MPs and Intermediates

Synthesis of CPT-Nva—The CPT-Nva prodrug was synthesized as described previously [27].

Preparation of PEGylated MPs (Compound 2)—The CPT-Nva conjugated PEGylated MPs were synthesized as shown in Figure 1. Carboxyl MPs (Compound **1**) were washed twice with double distilled water and dried under vacuum for 2 hours. The dried MPs were then suspended in anhydrous DMSO. To this suspension, DAPEG (2 eq) and DMAP (catalytic amount) in DMSO were added. DIPC (2 eq), was added to the reaction mixture. The progress of the PEGylated coupling to MPs was monitored using a Fluram test [28]. After completion of the reaction, the PEGylated MPs were washed with water and collected using centrifuge and dried under vacuum to yield the PEGylated MPs.

Preparation of EDTA coated PEGylated MPs (Compound 3)—The primary amine group on Compound **2** was converted to a carboxyl group upon the addition of EDTA to PEGylated MPs. EDTA (2 eq), DIPC (8 eq) and DMAP (4 eq) were mixed in DMSO in advance; the mixture was vigorously shaken to completely dissolve the EDTA. Well-suspended PEGylated MPs in anhydrous DMSO were added drop-wise to the EDTA mixture. The progress of the reaction was again monitored using a Fluram test. After completion of the reaction, the EDTA coated PEGylated MPs (Compound **3**) were washed with water, and collected by centrifugation and dried under vacuum to yield the EDTA coated PEGylated MPs (Compound **3**).

Synthesis of CPT-Nva-MPs Prodrugs (Compound 4)—CPT-Nva (1.2 eq), DIPC (1.3 eq) and DMAP (1 eq) were dissolved in DMSO (15 mL) and added drop-wise into well-suspended EDTA coated PEGylated MPs in DMSO. The reaction was stirred at room temperature. The progress of the reaction was monitored using a fluorescence microscope. The reaction was considered complete when the fluorescence intensity (because of CPT) of the MPs did not change over time. Upon completion of the reaction, CPT-Nva-MPs were washed three times with methanol to remove any unreacted CPT.

A549 cell culture

The human lung carcinoma cell line A549 (ATCC, Manassas, VA) was cultured in Dulbecco's Modified Eagle Medium: Nutrient Mixture F-12 (DMEM/F-12) 1:1 Mixture (Invitrogen®, Carlsbad, CA) supplemented with 10% fetal bovine serum, 100 U penicillin and 100 μg streptomycin at 37°C in a humidified atmosphere of 5% CO_2 in air. The cells were passaged when they reached 90% confluence.

Phagocytosis of CPT-Nva-MPs by A549 cells

A549 cells were seeded on Nunc Lab-Tek II Chamber slide system (Thermo Fisher Scientific, Rochester, New York, USA) at 5×10^4 cells/chamber, and were incubated overnight. Thereafter the carboxyl MPs, PEGylated MPs, and CPT-Nva-MPs (5 mg/ml suspended in cell culture medium) were added and incubated with the cells overnight. The cells were then rinsed three times with phosphate-buffered saline (PBS) and once with 0.2 M NaCl adjusted to pH 2.5 with acetic acid to remove nonspecifically bound MPs. After fixation with 4% formaldehyde for 30 minutes, cells were viewed under a phase contrast microscope. The fixed cells were further air-dried for SEM.

Pharmacokinetics of CPT-Nva-MPs

CPT was dissolved in DMSO (5 mg/mL) before dilution by Intralipid® to a final concentration of 2 mg/mL. CPT-Nva-MPs for injection were suspended in saline containing 0.1% Tween 80 (100 mg/mL) and were sonicated and vortexed immediately before injection to avoid particle aggregation.

Jugular vein cannulated Sprague Dawley rats (n=4) were injected with a single bolus dose of CPT (2 mg/kg) or CPT-Nva-MPs (100 mg/kg) through the tail vein. Blood was collected from a cannulated jugular vein at 0, 5, 10, 15, 30, 60 min, 2, 4, 8, 12, and 24 hours after CPT and CPT-Nva-MPs was administered to animals. Animals receiving CPT-Nva-MPs had additional blood samples collected at 36, 48, 60, 72, 84, and 96 hours after drug administration. The blood samples were placed on ice immediately after collection from the animals and were centrifuged at 12,000×g for 5 min at 4°C. The supernatants were stored at −20°C until analysis.

The plasma samples were deproteinized by mixing with three times volumes of ice-cold methanol. After centrifugation at 10,000×g for 5 min, the supernatants were mixed with

equal volume of 0.1N HCl. The total CPT released was analyzed using HPLC methods described below [29–32].

Analysis of CPT

The analysis of CPT was performed using a C-18 reverse phase column (Supelcosil™ LC-18, 4.6×330 mm) coupled with a C-18 guard column (Supelguard™ LC-18, 2.1×20 mm) on a Waters 2690 Alliance HPLC system (Waters Corp., Milford, MA). An isocratic mobile phase consisted of a mixture of 20% acetonitrile: water (20:80) containing 1% triethylamine/acetic acid (1:1) pH 4, at flow rate of 1 mL/min. The detection was performed using a fluorescence detector (Shimadzu Scientific Instruments Inc., Columbia, MO) with an excitation wavelength of 360 nm and an emission wavelength of 440 nm. The lower limit of detection for CPT was 0.1 ng/mL.

Orthotopic lung cancer rat model

An orthotopic animal model of human lung cancer in nude rats used in this study was previously established [33] and characterized [34]. Nude rats (200–250 g) were irradiated with 500 rads of whole-body gamma irradiation from a ^{127}Cs source. The radiation dose was sublethal for the purpose of immune suppression [35]. After 2–3 hours of resting, the animals were anesthetized using ketamine/xylazine and were placed supinely on a rodent operation board tilted at a 45° angle [36]. The maxilla was pulled down by using an elastic band to keep the mouth open. A light bulb (50 watt) was placed perpendicular to the animal's chest (~5 cm from the skin) to allow transillumination of the thorax. The trachea and epiglottis were made apparent by thoracic transillumination. A sterile, disposable and flexible 18-gauge feeding needle was passed through the illuminated vocal cord to the trachea, and 0.3 mL of 5×10^6 A549 cells suspension in serum-free medium was administered to the lung through the needle slowly. The ability to induce lung cancer in nude rats is close to 100% as demonstrated previously [34].

Maximum tolerated dose (MTD) study

It was previously determined by our group that the MTD of CPT for a single bolus intraperitoneal injection in rats was 5 mg/kg [37]. MTD was defined as a dose that caused no drug-related lethality and that produced no animal body weight loss more than 20% of the original animal weight. CPT at multiple doses (0.33, 0.56 and 0.83 mg CPT/kg) or single dose (1.11 mg CPT/kg), and CPT-Nva-MPs at multiple doses (5, 20, 50 and 150 mg MPs/kg MPs or 0.011, 0.044, 0.11, 0.33 mg CPT/kg, respectively), or single dose (250 mg MPs/kg or 0.55mg CPT/kg) were injected intravenously to Sprague Dawley male rats (n=3) every 3 days for 27 days. Body weight was monitored daily for the first week and 2– 3 times per week thereafter. At the end of the study, the lungs, liver, heart, kidneys, and spleen were removed and fixed with 10% neutral buffered formalin for hematoxylin and eosin (H&E) staining.

Anti-cancer efficacy of the CPT-Nva-MPs

One week after the A549 cell inoculation, nude rats (n=5) were injected with CPT-Nva-MPs (50 and 100 mg/kg, equivalent to CPT 0.11 mg/kg and 0.22 mg/kg), CPT (2 mg/kg) or vehicle control (saline containing 0.1% Tween 80). The treatment was conducted every 3 days for 27 days. The day after the last treatment, all animals were euthanized, and organs (lungs, liver, heart, kidneys, and spleen) were dissected and weighed. The organs were fixed in 10% neutral buffered formalin for H&E staining.

Stained lung sections were thoroughly examined under a light microscope coupled with a digital camera connected to a computer. Images of the sections with lung cancer sites were

captured and recorded. The images were further analyzed using ImageJ® v 1.32 (National Institutes of Health, USA, http://rsb.info.nih.gov/ij/) software. The number of tumor sites of each rat lung was recorded. The size of the lung cancer site was measured and analyzed using the ImageJ® software. The anti-cancer efficacy was evaluated based on the following four parameters: the number of rats found to be free of lung cancer, the average number of cancer sites in each treatment group, the average size of lung cancer sites in each treatment group, and the total area occupied by tumor cells. The toxicity of the treatments was evaluated by comparing the body weight changes of the rats in different treatment groups to those in the control group.

Statistical Analysis

Statistical analyses were performed using Microsoft Excel v.9.0 (Microsoft Corp.). The experimental values were expressed by mean ± standard deviation. Differences between experimental groups were tested using a t-test at $\alpha=0.05$. The significance of a single factor in groups was tested by analysis of variance (ANOVA) at $\alpha=0.05$. The regression analysis of the standard curves was performed using least squares linear regression (Microsoft Excel v.9.0) and nonlinear regression was performed using GraphPad Prism v.4 (GraphPad Software, Inc.). All the graphics were generated by GraphPad Prism v.4.

Results and Discussion

Analysis of CPT-Nva-MPs

The surface morphology of the CPT-Nva-MPs was examined by both light/fluorescence microscopy and SEM. The strong fluorescence under the microscope ($\lambda_{ex} = 360\pm40$ nm / $\lambda_{em} > 420$ nm) indicated good conjugation efficiency of CPT-Nva to the MPs (images not shown). There were no visible size differences between CPT-Nva-MPs and unmodified MPs. SEM micrographs of CPT-Nva-MPs are shown in Figure 2. CPT-Nva-MPs retained their spherical shape and surface morphology indicating that the synthesis schemes were suitable to the MPs. The size of the dry CPT-Nva-MPs was visually inspected under SEM and found to be the same as unmodified MPs.

The amount of bound CPT-Nva-MPs was determined by the release of CPT from CPT-Nva-MPs in phosphate buffer saline (PBS, pH 7.4) and in rat plasma at 37°C (Figures 3A and B, respectively). HPLC with fluorescence detection was used to identify the release of CPT from the MPs. Triethylamine acetate buffer was used in the mobile phase to serve as the ion-pairing reagent; provide an adequate retention of the carboxylate form of the drug; act as a masking reagent for underivatized silanols to prevent peak tailing; and to serve as the major buffer component [31].

The majority of CPT (~90%) was released from the MPs over a 24 hours period. The release of CPT, due to the hydrolysis of the ester bond, in rat plasma was much more rapid than in PBS suggesting the possible involvement of carboxylesterase and β-glucuronidase enzymes which are presents in rat plasma [38–40]. Furthermore, the release kinetics were found to follow first order in plasma ($R^2=0.9902$) and in PBS ($R^2=0.9823$). The amount of CPT contained in CPT-Nva-MPs was found to be 2.2 μg per mg of MPs.

Phagocytosis of MPs by the human lung carcinoma cell line, A549

The phagocytosis of 6 μm unmodified polystyrene MPs, PEGylated MPs, and CPT-Nva-MPs were evaluated in A549 cells. Polystyrene MPs are widely used to study phagocytosis [41–44] because they are commercially available with a narrow size distribution, are internally fluorescently labeled, have various functional groups on the MPs for further surface property modification, and have high stability in biological media relative to

biodegradable MPs. Since the goal of this study was to test the local release and conversion of the CPT prodrug and its effect on lung cancer when passive lung targeting was used, an inert nondegradable MP was the best choice to produce unbiased results. Since these initial studies, we have successfully synthesized biodegradable MPs. The SEM micrographs of the unmodified polystyrene MPs are shown in Figure 4. The process of phagocytosis was rapid, and occurred within 8 hours of incubation. It was observed that a single cancer cell was able to ingest one or more MPs. The ingested MPs were arranged in a way to minimize the space occupied inside the cell (Figure 4B). It is known that a macrophage is capable of ingesting a single particle ~1.5 times its diameter or 3 times its volume [44]. However, the ingestion capacity of epithelial cells or cancer cells is unknown. Since phagocytosis is not one of their primary physiological functions, it was surprising that a single A549 cell was able to take-up numerous MPs (Figure 4A–C), which occupied at least 700 to 850 μm^3 if the space between MPs were not considered. Thus, A549 cells could ingest comparable or greater amount of MPs than macrophages. A high magnification SEM micrograph (Figure 4C) shows that a single A549 cell in the process of 'ingesting' one of the unmodified MPs by engulfing the particle with its cell membrane. The intact cell membrane indicates that the cells were healthy. The current evidence does not support an alternative explanation to the apparent phagocytosis, as MPs were added after the attachment of A549 cells to the glass surface of the slides, it is very unlikely that the cells in Figure 4 are on top of the MPs. Before SEM, A549 cells were confluent (Figure 4A), the MPs were added to the monolayer of cells, and the incubation with the MPs lasted overnight. Therefore there was almost no chance that cells could grow on top of MPs. The inert MPs were obviously unable to migrate underneath the cells. Another alternative explanation is that the MPs are coated with layer of albumin or cellular protein(s). Although this possibility cannot be ruled out, it is also unlikely. Figure 4B presents a cluster of cells at a higher magnification. Except for two MPs (arrow-pointed), the MPs do not look like they are coated with a protein layer, because the contour of the layer over the MPs does not follow the shapes of individual MPs but assumes a cell membrane appearance with tight tension. In addition, the two MPs (indicated by an arrow) are not "coated", which is contrary to what would be expected by the "coating mechanism".

Interestingly, a similar result was obtained from cells treated with PEGylated MPs (data not shown). It is well known that the PEGylated particles possess "stealth" properties and thus are able to bypass uptake by macrophages [45–48]. Interestingly, the PEGylated MPs were not "stealthy" to cancer cells, perhaps this was due to the cationic surface charge of the MPs obtained after PEG modification. The cancer cells were able to recognize the PEGylated MPs and phagocytosize those as efficiently as unmodified MPs. The mechanism of MP phagocytosis might be different among cell types. For example, Foster et al. [42] demonstrated that the internalization of albumin-coated MPs by two epithelial cell lines, A549 and Calu-3, occurred as readily as for the uncoated ones. However, in a study using macrophages, neutrophils and monocytes, the phagocytosis of albumin-coated MPs was greatly reduced probably due to the fact that the reticuloendothelial system (RES) was not able to recognize the albumin-coated MPs as foreign matter [49, 50]. In the current study, significant differences were not observed in the uptake efficiency between non-modified polystyrene MPs and the PEGylated MPs by the epithelial cancer cells, A549. The differential uptake of PEGylated MPs by epithelial cell and macrophages could represent another important cancer targeting element for this drug delivery system.

The A549 cells were also capable of ingesting CPT-Nva-MPs (Figure 5A). Observation under fluorescent microscopy showed that significant amount of CPT was still bound to the MPs (Figure 5B). This is consistent with the *in vitro* stability study of the CPT-Nva-MPs (Figure 3A), where only ~10% of CPT was released after 8 hours of incubation in buffer. The cells were further examined by SEM after being air-dried and sputter coated with gold. This micrograph suggests that CPT-Nva-MPs were ingested by A549 cells (Figure 5C–D).

Interestingly, it was observed that a single cancer cell was also capable of ingesting multiple CPT-Nva-MPs. Under higher magnification (Figure 5D), we were able to visualize CPT-Nva-MPs in the process of being engulfed by a cell. However, the cell membrane of the cell that ingested CPT-Nva-MPs was obviously thinner than the one which ingested the unmodified MPs (Figure 4C) and lacked a distinctive membrane edge. In addition, it appears that A549 cells lose their ability to efficiently arrange the ingested CPT-Nva-MPs minimizing the space occupied as the cells did with the unmodified MPs.

Pharmacokinetics of CPT and CPT-Nva-MPs

Plasma concentrations of CPT were analyzed by HPLC after a single bolus IV injection of CPT-Nva-MPs and free CPT in rats. CPT plasma concentration is plotted as a function of time in Figure 6. Free CPT was rapidly excreted from the blood in a bi-exponential manner as reported by other groups [32, 51, 52]. However, CPT-Nva-MPs, had an initial increase in CPT plasma concentration with a t_{max} of 0.5 hour followed by an elimination phase to a barely detectable level at 24 hours. The small burst in systemic CPT plasma concentration after the administration of CPT-Nva-MPs is significantly lower than concentrations found initially following an IV bolus dose and more importantly, lower than the toxic threshold that is known to lead to severe systemic side effects in humans. The plasma concentration of CPT then gradually increased to a plateau with consistent concentrations of ~1 ng/mL until the end of study (96 hours). The constant CPT plasma concentration in the later phase after the administration of CPT-Nva-MPs was possibly due to the sustained release of CPT from the delivery system, as demonstrated in the *in vitro* stability study, where the half-life of CPT-Nva-MPs was in terms of days (Figure 3A and 3B). The reduction in CPT plasma concentrations after 6–8 hours corresponds well to the uptake and retention of MPs in pulmonary macrophages. Interestingly, the increase in CPT plasma concentrations at approximately 48 hours also roughly corresponds with our previous results demonstrating that MPs of this size are transiently retained in the lung for 24–48 hours. This would suggest that during this period of time, higher local CPT concentrations were being achieved. Given the treatment regimen employed in this study (a single injection once every three days), it is reasonable to expect that local but high CPT concentrations were maintained for the duration of the study while highly fluctuating and transient concentrations would be observed after IV injection of free CPT.

Maximum tolerated dose of MPs

No noticeable side effects were observed in any of the rats regardless of the amount of CPT administered for all treatments. However, the average increase in body weight of CPT treated group was lower than the control group indicating that the animals might be suffering from a loss of appetite while receiving treatment (Figure 7A). One rat receiving 250 mg/kg of CPT-Nva-MPs displayed symptoms of embolism immediately after the first injection. The animal was promptly euthanized to avoid unnecessary suffering. Rats administered with 150 and 50 mg/kg of CPT-Nva-MPs showed no signs of side effects (including embolism) throughout the study. Over the course of the study, rats injected with 150 mg/kg or 50 mg/kg CPT-Nva-MPs received total doses of 1350 and 450 mg/kg, respectively, which were 5.4 and 1.8 fold greater than the acute lethal dose of 250 mg/kg.

Animals receiving CPT-Nva-MPs had body weight increases similar to the control group except for animals receiving 150 mg/kg (Figure7B). Gross examination of the lung, liver, spleen and kidney of animals receiving 150 mg/kg of CPT-Nva-MPs observed enlarged spleens, which were 3-fold larger in weight than control groups. MPs accumulation in the spleen resulted because of the non-biodegradable nature of polystyrene MPs. In addition to the spleen, accumulated MP were observed in histological sections of lung tissue from rats treated with multiple doses of 50 mg/kg (Figure 8A and B) and 150 mg/kg (Figure 8C and

D). The MPs were observed to a lesser extent in the lungs from rats receiving multiple doses of 50 mg/kg CPT-Nva-MPs (Figure 8A and B) compared with and 150 mg/kg (Figure 8C and D). Therefore, it was determined that 150 mg/kg of CPT-Nva-MPs was a toxic, but not lethal dose, and 50 mg/kg was a non-toxic dose. The highest dose of CPT tested did not reach the MTD of 5 mg/ml via intraperitoneal administration determined previously by our group [37]. Rats administered 50 mg/kg CPT-Nva-MPs with a total dose of 450 mg/kg did not show any signs of toxicity under gross and histological inspection of blood-pooled organs. Animals administered 150 mg/kg (total dose of 1350 mg/kg) of CPT-Nva-MPs did not show any signs of distress or embolism during the experiment, although the increase of body weight was less than rats in other groups. Histological examination showed the enlarged spleen indicated the accumulation of non-degradable MPs after they were cleared from the lungs (data not shown). Therefore, two doses (100 mg/kg and 50 mg/kg) of MPs were chosen for the anti-cancer efficacy studies.

Anti-Cancer Efficacy of the CPT Conjugated MPs

Nude rats bearing A549 tumor in lung (n=5) were treated with CPT-Nva-MPs (100 mg/kg and 50 mg/kg), CPT (2 mg/kg) or saline containing 0.1% Tween 80 (as vehicle control group) one week after the inoculation of lung cancer. The treatment was applied once every 3 days for 27 days. Anti-cancer efficacy was evaluated by examining the following three factors: the average tumor size; the average number of tumor sites; and the total area occupied by tumor cells found in the lung tissue samples. The total area occupied by tumor cells was calculated by multiplying the average number of tumor sites and the average size of tumor sites found in the lung tissue (Figure 9). Animals receiving 100 mg/kg of CPT-Nva-MPs had the fewest number of cancer sites, average cancer site size, and area occupied by tumor cells. In addition to the lower number of cancer sites found and smaller area occupied by cancer cells, 40% of the animals receiving 100 mg/kg of CPT-Nva-MPs inoculated with lung cancer cells were found to be free of cancer, while tumor sites were found in all animals in other treatment groups. The largest average number of cancer sites found in the lung tissue occurred in control group, followed by groups receiving 50 mg/kg of CPT-Nva-MPs, 2 mg/kg of CPT, and 100 mg/kg of CPT-Nva-MPs, respectively. The CPT dose of CPT-Nva-MPs (100 mg/kg) was ten fold lower than after IV injection of free CPT but was found to be more effective in reducing the amount of cancerous areas. The largest average cancer site size found in the lung tissue occurred in control animals followed by 2 mg/kg of CPT, 50 mg/kg of CPT-Nva-MPs, and 100 mg/kg of CPT-Nva-MPs, respectively. The result of the statistical analysis suggests that the average size of cancer sites found in the lung tissue from the animals receiving 100 mg/kg of CPT-Nva-MPs was significantly ($P < 0.05$) lower than that of the control group.

All animals lost weight after the inoculation of lung cancer cells, and recovered before the initiation of treatment (Figure 10). The decrease in body weight was most likely due to distress caused by irradiation, anesthesia and/or liquid in the lungs. The change in body weights in all groups was not significantly different from each other indicating that the doses of free CPT and CPT-Nva-MPs administered were well tolerated. The analysis of the data shows that, animals receiving the 100 mg/kg dose of CPT-Nva-MPs had the largest increase in body weight among all treatment groups. The absence of signs of toxicity from all treatments was confirmed in a pharmacokinetic analysis of plasma CPT. None of the animals died due to the cancer burden or treatment toxicity during the study period.

Although plasma CPT concentrations from rats receiving CPT-Nva-MPs were constant and significantly lower than that of rats receiving free CPT, the anti-cancer efficacy was superior. We hypothesize that after the delivery system was entrapped in the lung tissue, the majority of the MPs were phagocytosed by the A549 cells or the alveolar macrophages while the CPT was still covalently bound to the MPs. The hydrolysis of the ester bond

occurred intracellularly, resulting in cell death. Only small portions of the CPT-Nva-MPs, which bypass pulmonary filtration and phagocytosis by macrophages, were able to release free CPT into the general circulation. In our previously published work, we reported that camptothecin is a substrate of MRP2, and Pgp/BCRP through the use of inhibitors MK571 and GF120918 [53]. A549 cells are known to have high amounts of MRP2 mRNA and protein expression [54], however the amount of Pgp found in A549 cells is negligible suggesting that camptothecin could have been effluxed from A549 cells during the study by MRP2.

As a result, plasma CPT concentrations were constantly low. The decrease in nondetectable CPT concentrations from approximately 6 to 48 hours corresponds well with entrapment in the lung followed by release back into the system.

In conclusion, the current results demonstrate the feasibility of using a passive lung targeting approach with improved anti-cancer efficacy at ten times lower CPT doses and resulting in lower systemic concentrations and toxicity. However, although feasibility of the approach was readily demonstrated in the current study, polystyrene MPs cannot be used in humans since they cannot be eliminated from the body. Thus, the development of MPs using biocompatible materials is required. Our group's current efforts have focused on the design and development of biocompatible aggregated nanogel particles (ANPs). These particles were prepared using PEG and initial biodistribution studies shows that these particles are retained in the body for more than 24 hours and are predominately found in the lung. These particles will be an excellent alternative in order to replace polystyrene particles.

Acknowledgments

References

1. Jemal A, Siegel R, Ward E, Murray T, Xu J, Thun MJ. Cancer statistics, 2007. CA Cancer J Clin. 2007; 57:43–66. [PubMed: 17237035]

2. Travis WD, Lubin J, Ries L, Devesa S. United States lung carcinoma incidence trends: declining for most histologic types among males, increasing among females. Cancer. 1996; 77:2464–2470. [PubMed: 8640694]

3. Giaccone G, Pinedo HM. Drug Resistance. Oncologist. 1996; 1:82–87. [PubMed: 10387972]

4. Szakacs G, Paterson JK, Ludwig JA, Booth-Genthe C, Gottesman MM. Targeting multidrug resistance in cancer. Nat Rev Drug Discov. 2006; 5:219–234. [PubMed: 16518375]

5. Folkman J. Role of angiogenesis in tumor growth and metastasis. Semin Oncol. 2002; 29:15–18. [PubMed: 12516034]

6. Ferreira CG, Huisman C, Giaccone G. Novel approaches to the treatment of non-small cell lung cancer. Crit Rev Oncol Hematol. 2002; 41:57–77. [PubMed: 11796232]

7. Gatzemeier U, Pluzanska A, Szczesna A, Kaukel E, Roubec J, De Rosa F, et al. Phase III study of erlotinib in combination with cisplatin and gemcitabine in advanced non-small-cell lung cancer: the Tarceva Lung Cancer Investigation Trial. J Clin Oncol. 2007; 25:1545–1552. [PubMed: 17442998]

8. Giaccone G, Herbst RS, Manegold C, Scagliotti G, Rosell R, Miller V, et al. Gefitinib in combination with gemcitabine and cisplatin in advanced non-small-cell lung cancer: a phase III trial--INTACT 1. J Clin Oncol. 2004; 22:777–784. [PubMed: 14990632]

9. Herbst RS, Prager D, Hermann R, Fehrenbacher L, Johnson BE, Sandler A, et al. TRIBUTE: a phase III trial of erlotinib hydrochloride (OSI-774) combined with carboplatin and paclitaxel chemotherapy in advanced non-small-cell lung cancer. J Clin Oncol. 2005; 23:5892–5899. [PubMed: 16043829]

10. Herbst RS, Giaccone G, Schiller JH, Natale RB, Miller V, Manegold C, et al. Gefitinib in combination with paclitaxel and carboplatin in advanced non-small-cell lung cancer: a phase III trial--INTACT 2. J Clin Oncol. 2004; 22:785–794. [PubMed: 14990633]

11. Cabebe E, Wakelee H. Role of anti-angiogenesis agents in treating NSCLC: focus on bevacizumab and VEGFR tyrosine kinase inhibitors. Curr Treat Options Oncol. 2007; 8:15–27. [PubMed: 17634832]

12. Kutscher HL, Chao P, Deshmukh M, Singh Y, Hu P, Joseph LB, et al. Threshold size for optimal passive pulmonary targeting and retention of rigid microparticles in rats. *in preparation* PMID: 20043961.

13. Brewer J, Dunning J. An in vitro and in vivo study of glass particles in ampules. J Am Pharmacol Assoc. 1947; 36:289–293.

14. Kanke M, Simmons GH, Weiss DL, Bivins BA, DeLuca PP. Clearance of 141Ce-labeled microspheres from blood and distribution in specific organs following intravenous and intraarterial administration in beagle dogs. J Pharm Sci. 1980; 69:755–762. [PubMed: 7391933]

15. Prinzmetal M, Ornitz EM JR, Simkin B, Bergman HC. Arterio-venous Anastomoses in Liver, Spleen, and Lungs. Am J Physiol. 1947; 152:48–52. [PubMed: 18903426]

16. Scheffel U, Rhodes BA, Natarajan TK, Wagner HN Jr. Albumin microspheres for study of the reticuloendothelial system. J Nucl Med. 1972; 13:498–503. [PubMed: 5033902]

17. Schroeder HG, Simmons GH, DeLuca PP. Distribution of radiolabeled subvisible microspheres after intravenous administration to beagle dogs. J Pharm Sci. 1978; 67:504–507. [PubMed: 641758]

18. Niden A, Aviado D. Effects of Pulmonary Embolism on the Pulmonary Circulation With Special Reference to Arteriovenous Shunts in the Lung. Circulation Research. 1956; 4:67–73. [PubMed: 13277112]

19. Presson RG Jr, Todoran TM, De Witt BJ, McMurtry IF, Wagner WW Jr. Capillary recruitment and transit time in the rat lung. J Appl Physiol. 1997; 83:543–549. [PubMed: 9262451]

20. Colombetti LG, Moerlien S, Pinsky S. Rapid and reliable preparation of macroaggregated albumin suitable for lung scintigraphy. Int J Nucl Med Biol. 1975; 2:180–184. [PubMed: 1205665]

21. Hapke EJ, Pederson HJ. Ultrastructural changes in rat lungs induced by radioactive macroaggregated albumin. Am Rev Respir Dis. 1969; 100:194–205. [PubMed: 5805262]

22. Stauber RE, Mochizuki T, Van Thiel DH, Tauxe WN. The use of quantitative scintigraphy in the measurement of portal-systemic shunting in rats. Ann Nucl Med. 1992; 6:209–214. [PubMed: 1489630]

23. DeLand FH. The fate of macroaggregated albumin used in lung scanning. J Nucl Med. 1966; 7:883–895. [PubMed: 4163391]

24. McGhee JR, Czerkinsky C, Mestecky. J. Mucosal Vaccines: Overview. Mucosal Vaccines: Overview. 1999:741–757.

25. Taplin GV, Johnson DE, Kennady JC, Dore EK, Poe ND, Swanson LA, et al. Aggregated Albumin Labeled with Various Radioisotopes. Aggregated Albumin Labeled with Various Radioisotopes. 1966:525–551.

26. DeNardo GL, Goodwin DA, Ravasini R, Dietrich PA. The ventilatory lung scan in the diagnosis of pulmonary embolism. N Engl J Med. 1970; 282:1334–1336. [PubMed: 5444646]

27. Deshmukh M, Chao P, Kutscher HK, Laskin DL, Stein S, Sinko PJ. A series of -Amino Acid Ester Prodrugs of Camptothecin: In Vitro Hydrolysis and Cytotoxicity on Human Lung Carcinoma Cell. *in preparation* PMID:20063889.

28. Udenfriend S, Stein S, Bohlen P, Dairman W, Leimgruber W, Weigele M. Fluorescamine: a reagent for assay of amino acids, peptides, proteins, and primary amines in the picomole range. Science. 1972; 178:871–872. [PubMed: 5085985]

29. Ahmed F, Vyas V, Saleem A, Li XG, Zamek R, Cornfield A, et al. High-performance liquid chromatographic quantitation of total and lactone 20(S)camptothecin in patients receiving oral 20(S)camptothecin. J Chromatogr B Biomed Sci Appl. 1998; 707:227–233. [PubMed: 9613954]

30. Warner DL, Burke TG. Simple and versatile high-performance liquid chromatographic method for the simultaneous quantitation of the lactone and carboxylate forms of camptothecin anticancer drugs. J Chromatogr B Biomed Sci Appl. 1997; 691:161–171. [PubMed: 9140770]

31. Palumbo M, Sissi C, Gatto B, Moro S, Zagotto G. Quantitation of camptothecin and related compounds. J Chromatogr B Biomed Sci Appl. 2001; 764:121–140. [PubMed: 11817024]

32. Scott DO, Bindra DS, Stella VJ. Plasma pharmacokinetics of lactone and carboxylate forms of 20(S)-camptothecin in anesthetized rats. Pharm Res. 1993; 10:1451–1457. [PubMed: 8272406]

33. Johnston MR, Mullen JB, Pagura ME, Howard RB. Validation of an orthotopic model of human lung cancer with regional and systemic metastases. Ann Thorac Surg. 2001; 71:1120–1125. [PubMed: 11308147]

34. March TH, Marron-Terada PG, Belinsky SA. Refinement of an orthotopic lung cancer model in the nude rat. Vet Pathol. 2001; 38:483–490. [PubMed: 11572555]

35. Howard RB, Chu H, Zeligman BE, Marcell T, Bunn PA, McLemore TL, et al. Irradiated nude rat model for orthotopic human lung cancers. Cancer Res. 1991; 51:3274–3280. [PubMed: 2040002]

36. Cambron H, Latulippe JF, Nguyen T, Cartier R. Orotracheal intubation of rats by transillumination. Lab Anim Sci. 1995; 45:303–304. [PubMed: 7650904]

37. Paranjpe PV, Chen Y, Kholodovych V, Welsh W, Stein S, Sinko PJ. Tumor-targeted bioconjugate based delivery of camptothecin: design, synthesis and in vitro evaluation. J Control Release. 2004; 100:275–292. [PubMed: 15544875]

38. Tsuji T, Kaneda N, Kado K, Yokokura T, Yoshimoto T, Tsuru D. CPT-11 converting enzyme from rat serum: purification and some properties. J Pharmacobiodyn. 1991; 14:341–349. [PubMed: 1783980]

39. Kaneda N, Kurita A, Hosokawa Y, Yokokura T, Awazu S. Intravenous administration of irinotecan elevates the blood beta-glucuronidase activity in rats. Cancer Res. 1997; 57:5305–5308. [PubMed: 9393754]

40. Kurita A, Kaneda N. High-performance liquid chromatographic method for the simultaneous determination of the camptothecin derivative irinotecan hydrochloride, CPT-11, and its metabolites SN-38 and SN-38 glucuronide in rat plasma with a fully automated on-line solid-phase extraction system, PROSPEKT. J Chromatogr B Biomed Sci Appl. 1999; 724:335–344. [PubMed: 10219676]

41. Muller RH, Ruhl D, Luck M, Paulke BR. Influence of fluorescent labelling of polystyrene particles on phagocytic uptake, surface hydrophobicity, and plasma protein adsorption. Pharm Res. 1997; 14:18–24. [PubMed: 9034216]

42. Foster KA, Yazdanian M, Audus KL. Microparticulate uptake mechanisms of in-vitro cell culture models of the respiratory epithelium. J Pharm Pharmacol. 2001; 53:57–66. [PubMed: 11206193]

43. Thiele L, Rothen-Rutishauser B, Jilek S, Wunderli-Allenspach H, Merkle HP, Walter E. Evaluation of particle uptake in human blood monocyte-derived cells in vitro. Does phagocytosis activity of dendritic cells measure up with macrophages? J Control Release. 2001; 76:59–71. [PubMed: 11532313]

44. Cannon GJ, Swanson JA. The macrophage capacity for phagocytosis. J Cell Sci. 1992; 101(Pt 4): 907–913. [PubMed: 1527185]

45. Gref R, Minamitake Y, Peracchia MT, Trubetskoy V, Torchilin V, Langer R. Biodegradable long-circulating polymeric nanospheres. Science. 1994; 263:1600–1603. [PubMed: 8128245]

46. Dunn SE, Brindley A, Davis SS, Davies MC, Illum L. Polystyrene-poly (ethylene glycol) (PS-PEG2000) particles as model systems for site specific drug delivery. 2. The effect of PEG surface density on the in vitro cell interaction and in vivo biodistribution. Pharm Res. 1994; 11:1016–1022. [PubMed: 7937542]

47. Moghimi SM. Chemical camouflage of nanospheres with a poorly reactive surface: towards development of stealth and target-specific nanocarriers. Biochim Biophys Acta. 2002; 1590:131–139. [PubMed: 12063176]

48. Stolnik S, Dunn SE, Garnett MC, Davies MC, Coombes AG, Taylor DC, et al. Surface modification of poly(lactide-co-glycolide) nanospheres by biodegradable poly(lactide)-poly(ethylene glycol) copolymers. Pharm Res. 1994; 11:1800–1808. [PubMed: 7899246]

49. Ayhan H, Tuncel A, Bor N, Piskin E. Phagocytosis of monosize polystyrene-based microspheres having different size and surface properties. J Biomater Sci Polym Ed. 1995; 7:329–342. [PubMed: 7495763]

50. Roser M, Fischer D, Kissel T. Surface-modified biodegradable albumin nano-and microspheres. II: effect of surface charges on in vitro phagocytosis and biodistribution in rats. Eur J Pharm Biopharm. 1998; 46:255–263. [PubMed: 9885296]

51. Schluep T, Cheng J, Khin KT, Davis ME. Pharmacokinetics and biodistribution of the camptothecin-polymer conjugate IT-101 in rats and tumor-bearing mice. Cancer Chemother Pharmacol. 2006; 57:654–662. [PubMed: 16133526]

52. Tsai TH, Chen YF, Chou CJ, Chen CF. Measurement and pharmacokinetics of unbound 20(S)-camptothecin in rat blood and brain by microdialysis coupled to microbore liquid chromatography with fluorescence detection. J Chromatogr A. 2000; 870:221–226. [PubMed: 10722080]

53. Lalloo AK, Luo FR, Guo A, Paranjpe PV, Lee SH, Vyas V, et al. Membrane transport of camptothecin: facilitation by human P-glycoprotein (ABCB1) and multidrug resistance protein 2 (ABCC2). BMC Med. 2004; 2:16. [PubMed: 15125776]

54. Torky AR, Stehfest E, Viehweger K, Taege C, Foth H. Immuno-histochemical detection of MRPs in human lung cells in culture. Toxicology. 2005; 207:437–450. [PubMed: 15664271]
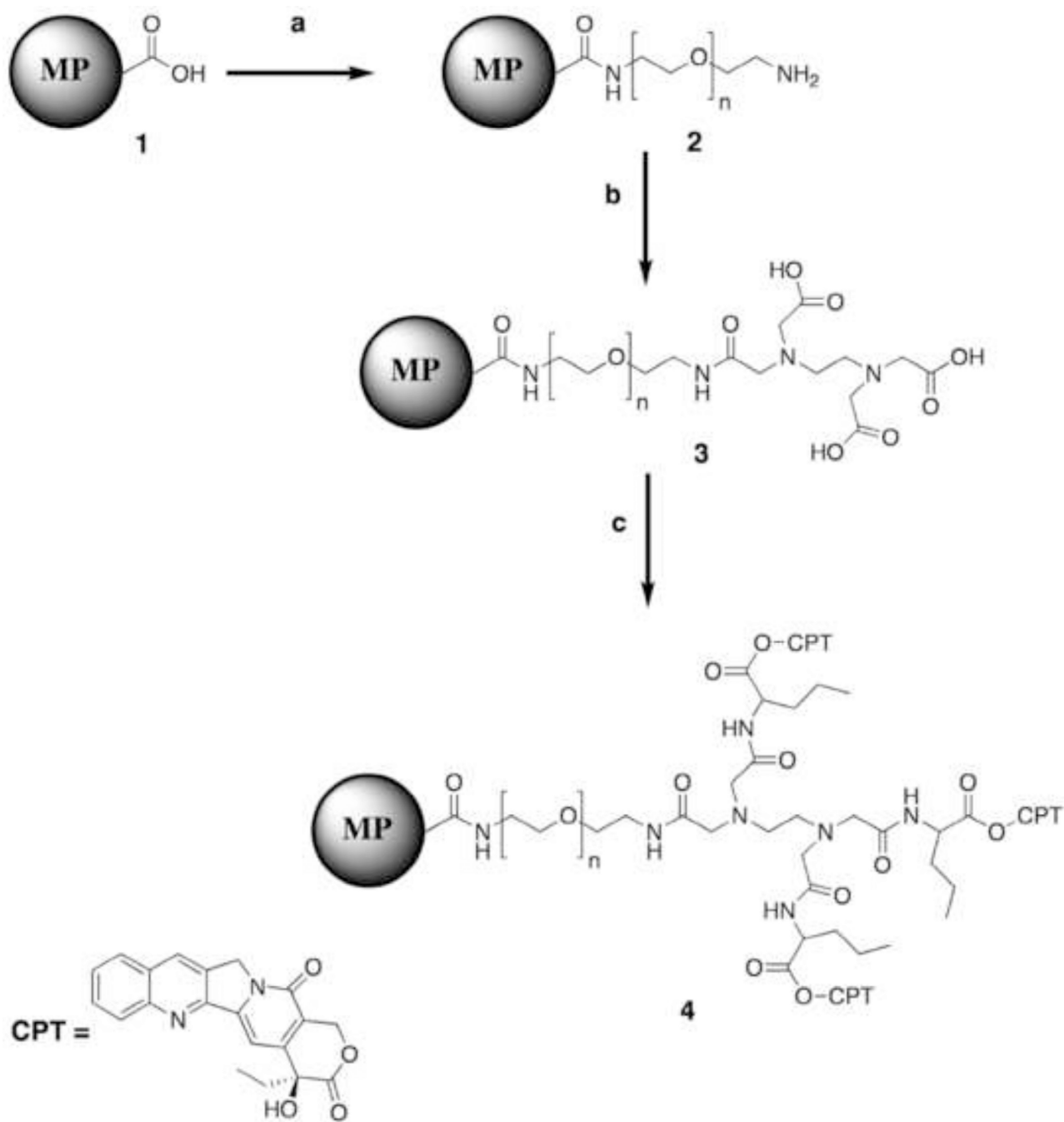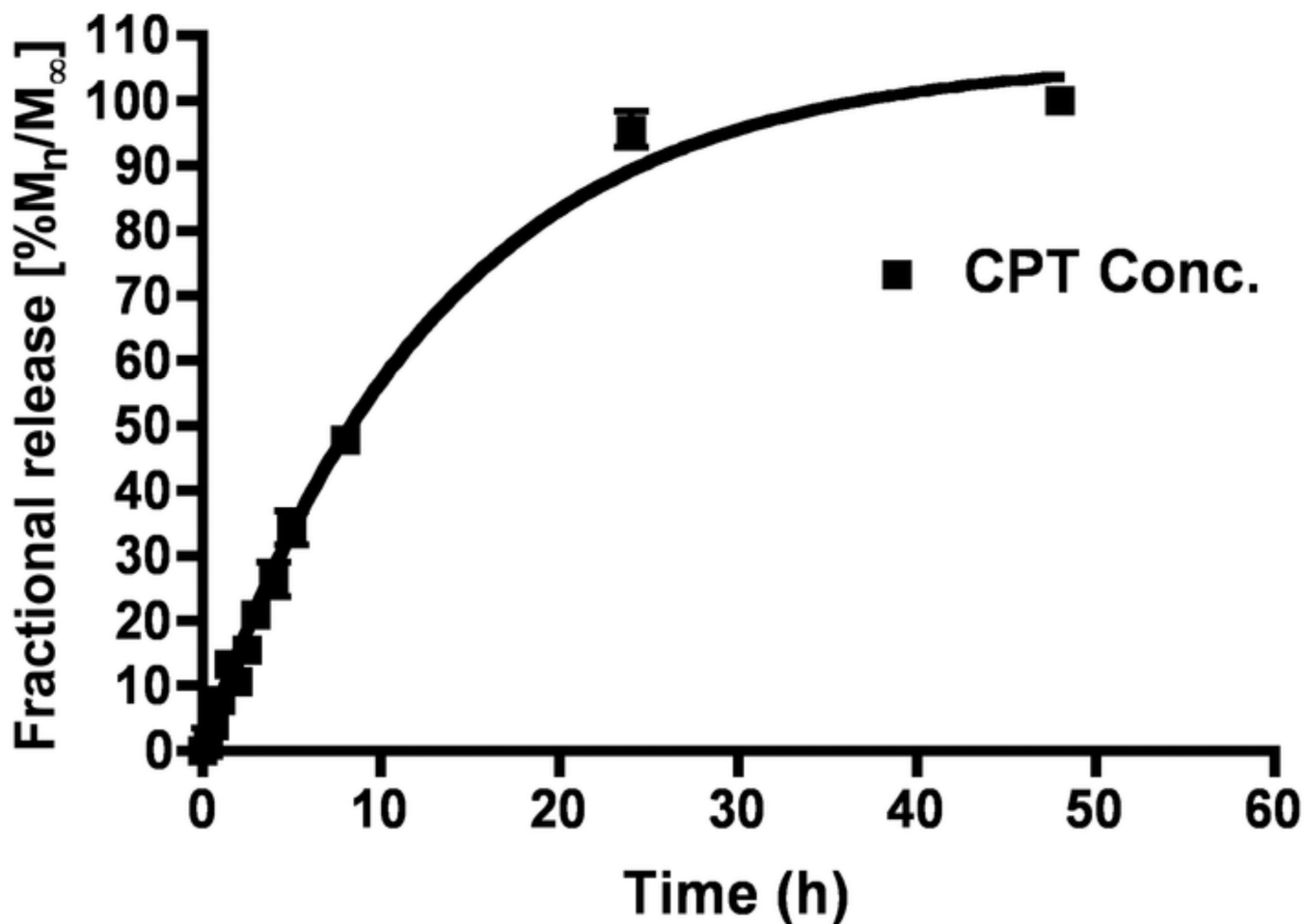
Figure 1.
Reaction performed for the synthesis of CPT-Nva-MPs reagents used; a) DAPEG (3.4kDa), DMAP, DMSO, room temperature; b) EDTA, DIPC, DMAP, DMSO, room temperature. c) Nva-CPT, DIPC, DMAP, DMSO, room temperature.
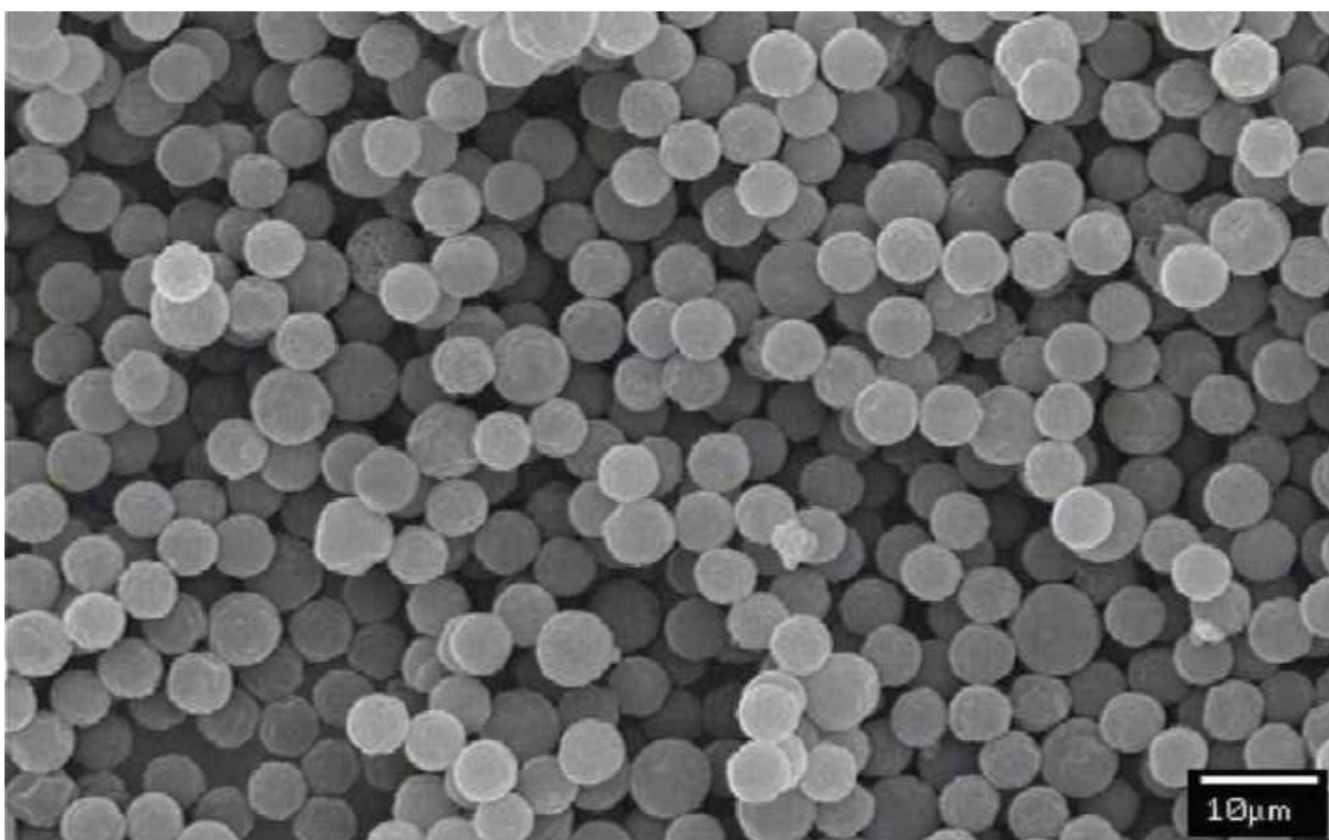
Figure 2.
SEM micrograph of CPT conjugated microspheres with amino acid linker CPT-Nva-MPs.
All of the microspheres showed an intact surface and spherical morphology indicating that
the modified synthetic procedure had little effect on the microspheres (bar = 10 μm).
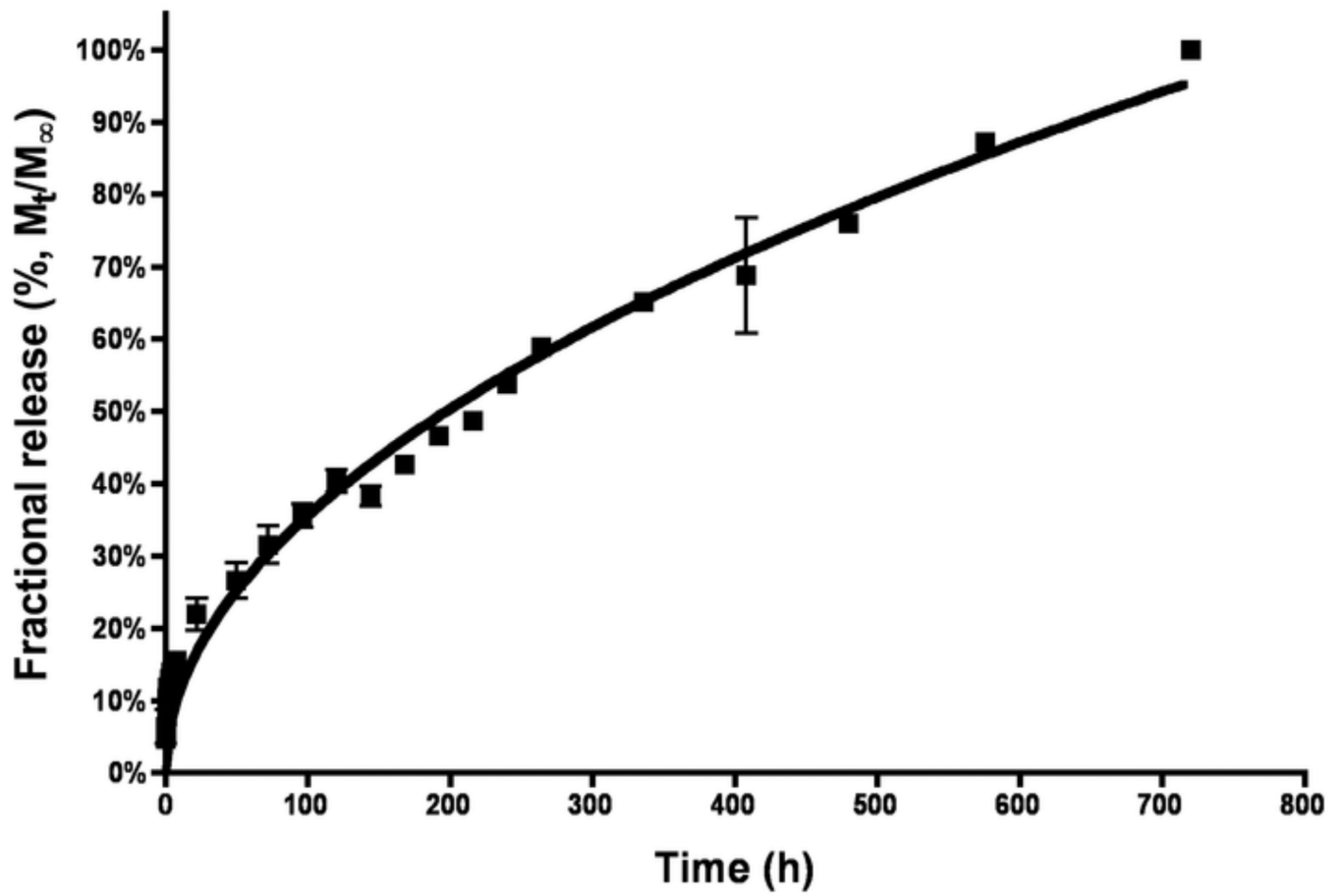
Figure 3.
A. Release of camptothecin from CPT-Nva-MPs in PBS (pH 7.4) solution at 370°C. First order release kinetics was initially observed (R^2 = 0.9823).
B. The release of camptothecin from CPT-Nva-MPs in rat plasma at 37°C. The line represents the best-fit line as determined by linear regression of the data. First order release kinetics was observed (R^2 0.9902).
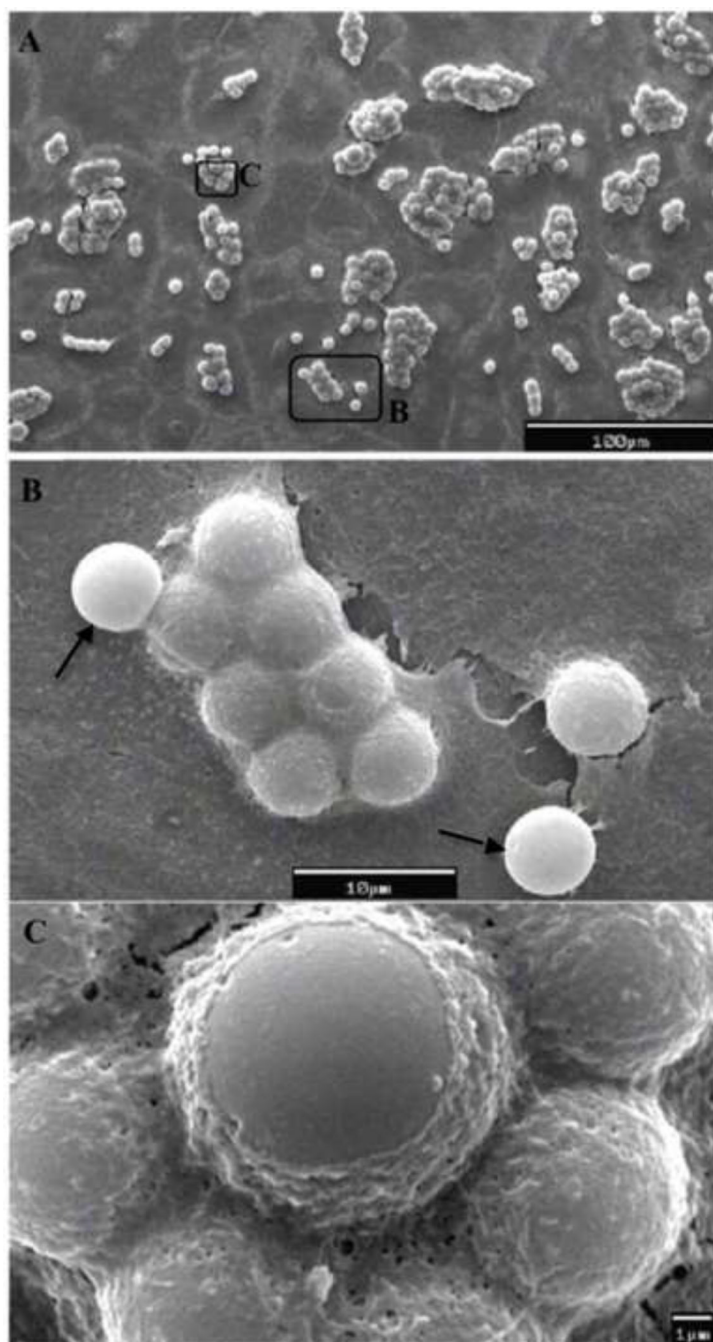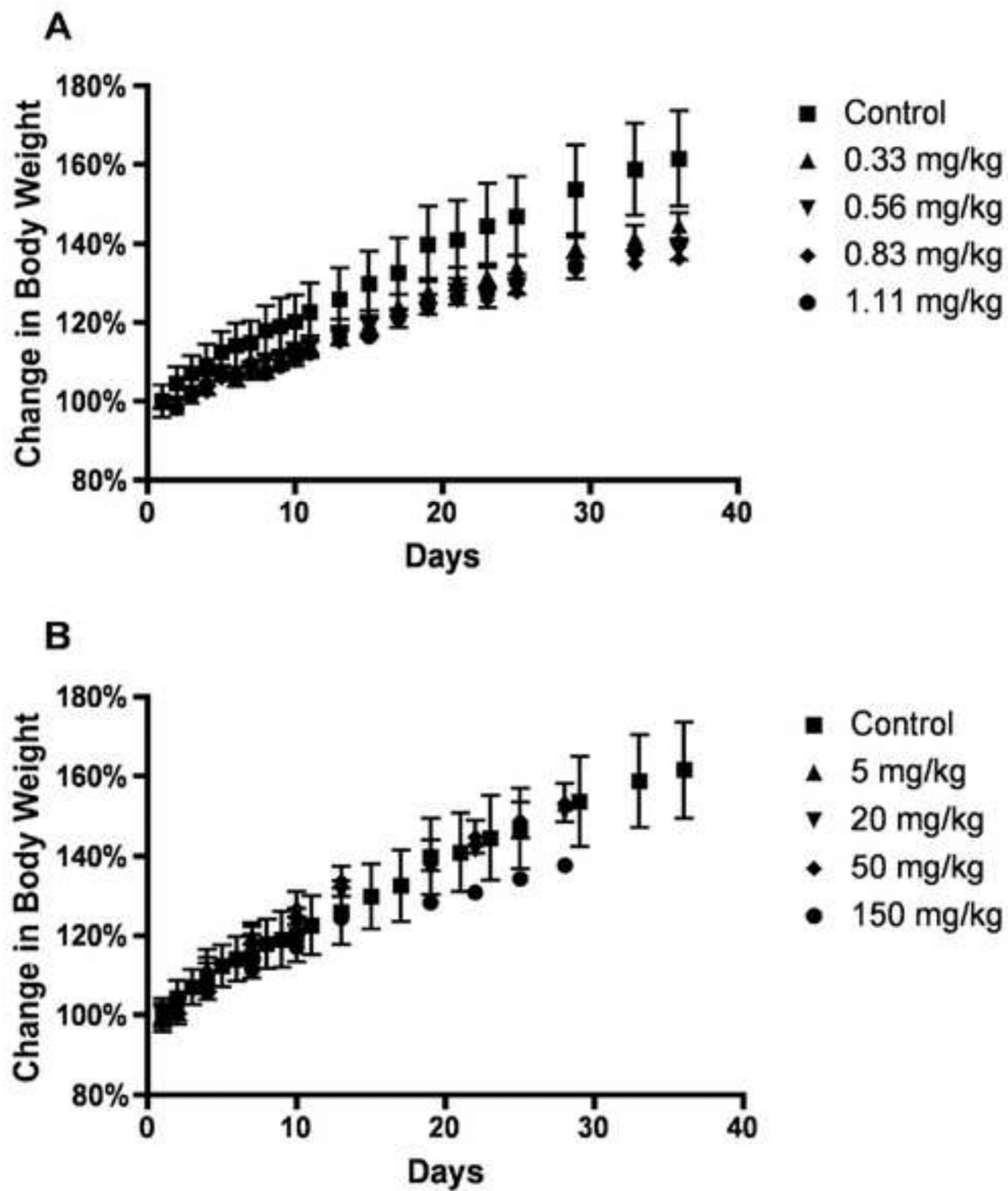
Figure 4.
SEM micrographs of the phagocytosis of 6μm unmodified carboxyl polystyrene MPs (A to C) by the human lung carcinoma cell line, A549.
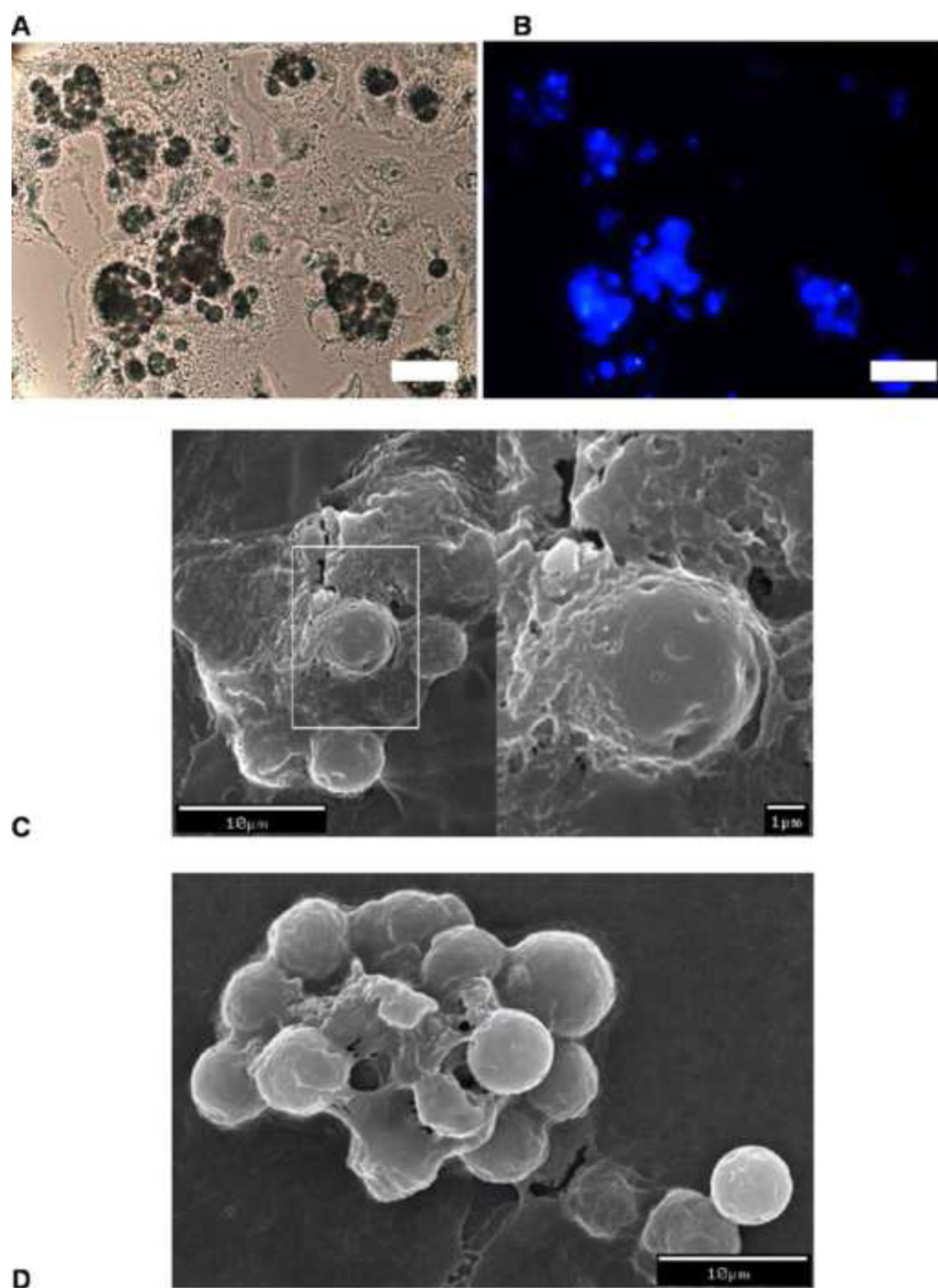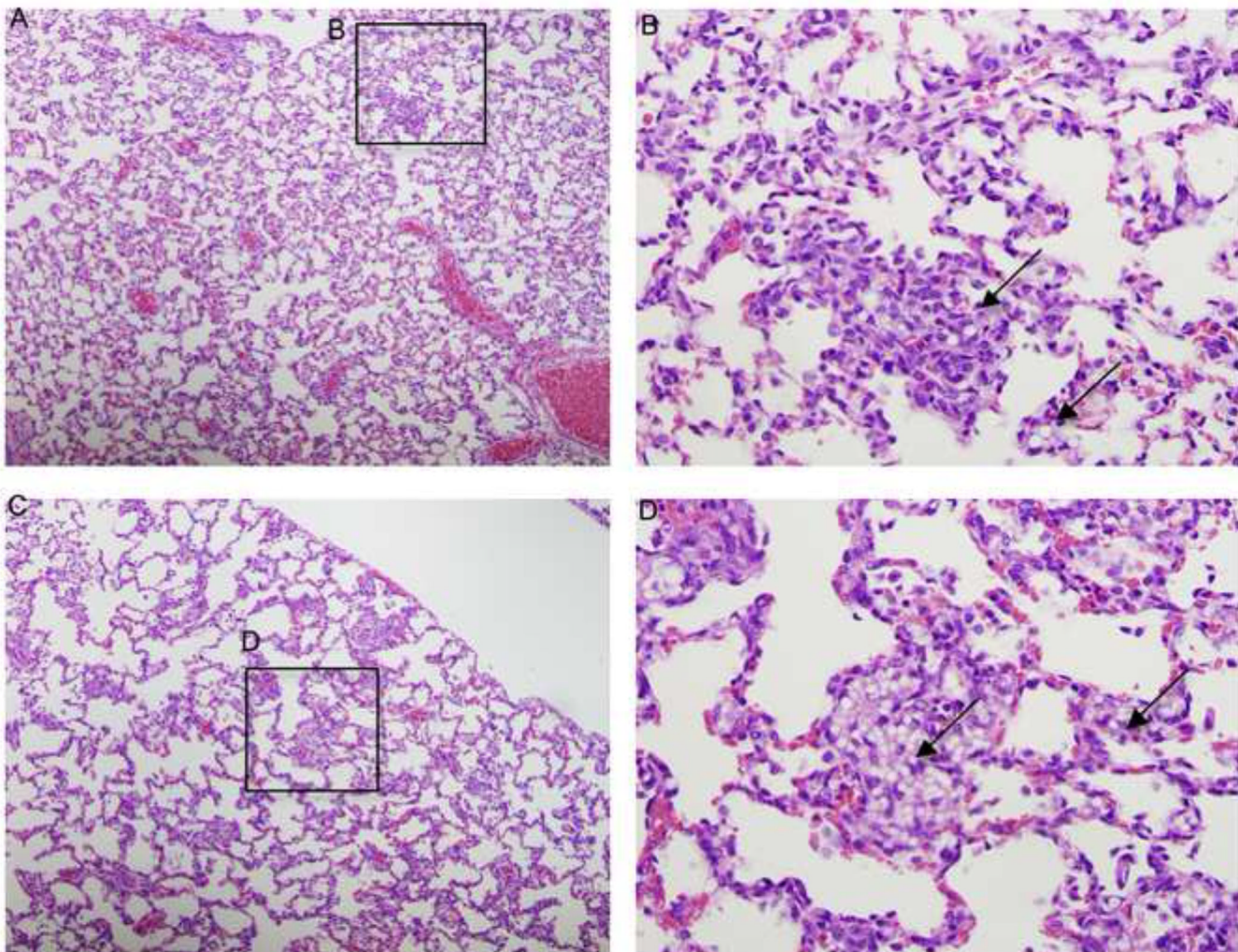
Figure 5.
Microscopy of the phagocytosis of CPT-Nva-MPs by A549 cells. A: light microscopy showing CPT-Nva-MPs aggregates inside the cells, B: the fluorescent microscopy of the same field as A (x 40, bar = 25 μm), C and D: SEM of the phagocytosis of CPT-Nva-MPs by A549 cells.
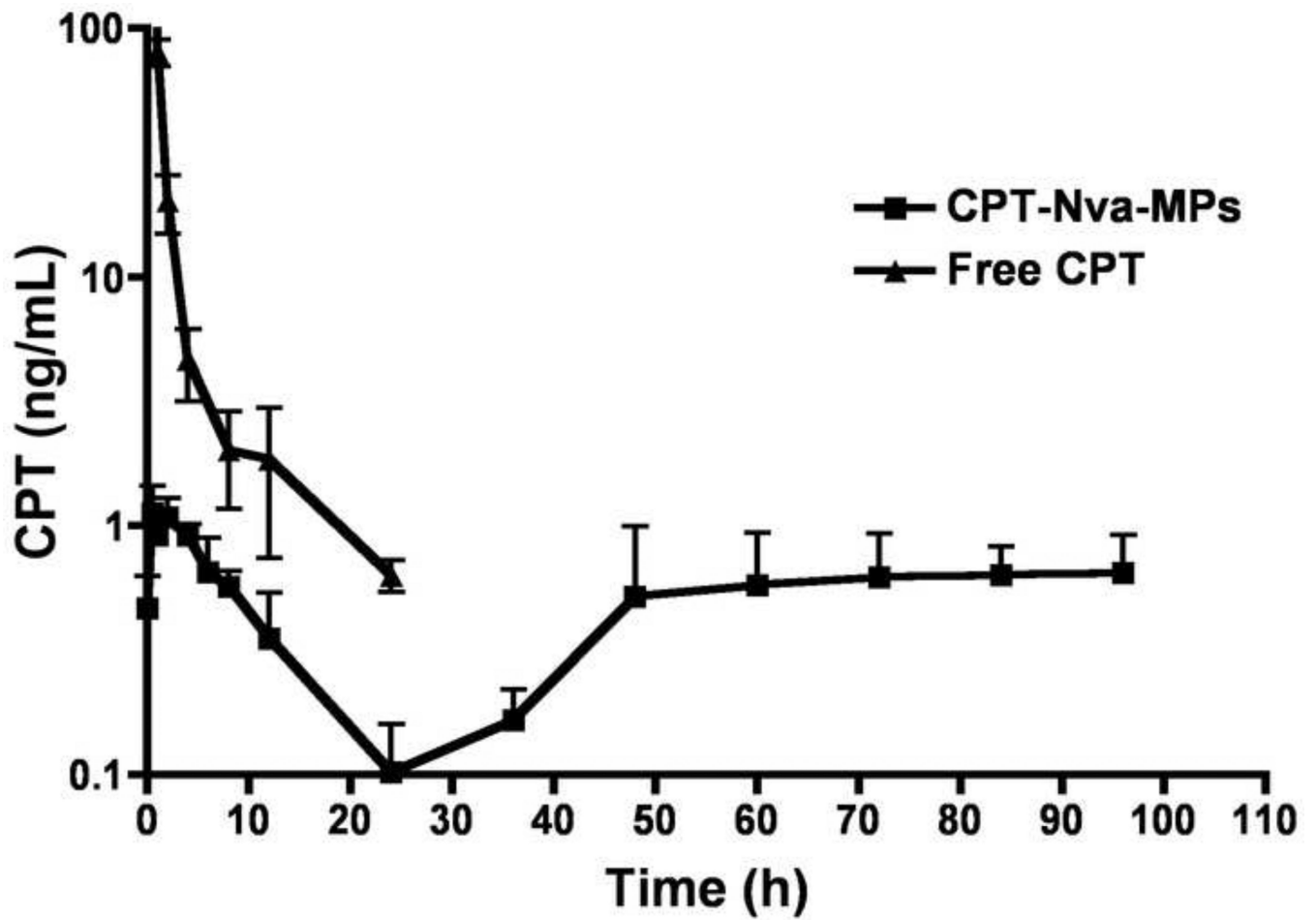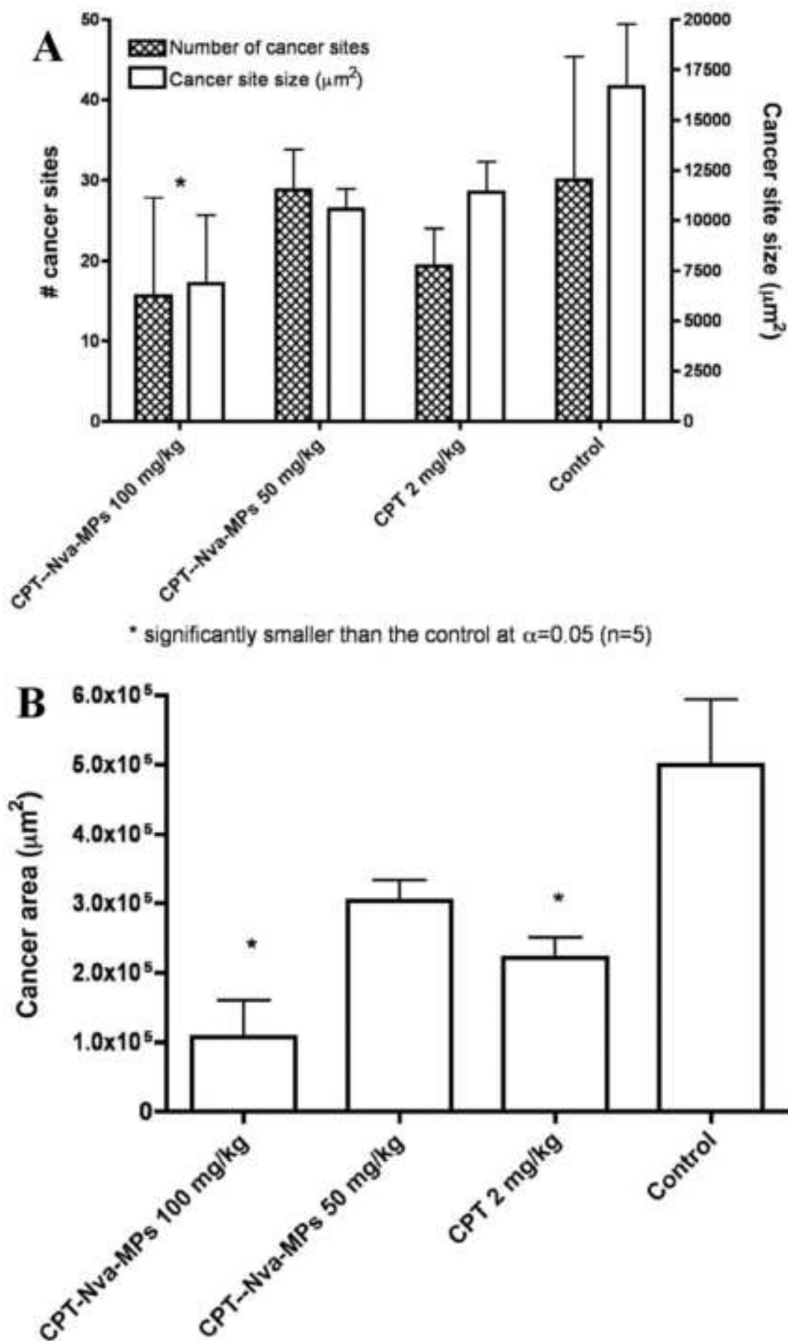
Figure 6.
Plasma concentration of CPT as a function of times it is plotted with mean +/−SEM after a single bolus i.v. injection of CPT-Nva-MPs (squares) and free CPT (triangles)

Figure 7.
(A) Maximum tolerated dose (MTD) studies obtained by change in body weight of multiple intravenous injections of free CPT and (B) CPT-Nva-MPs in Sprague Dawley rats.
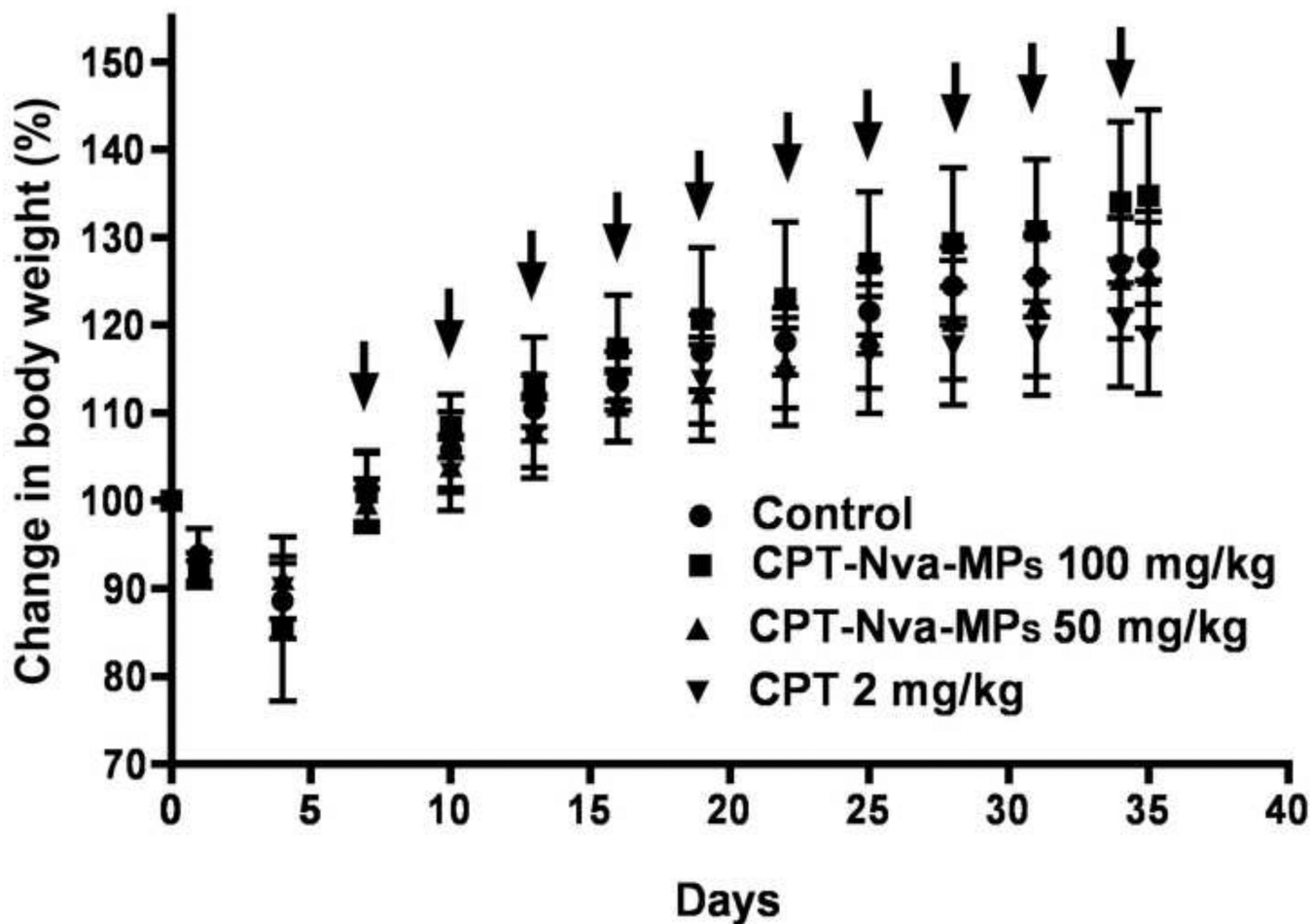
Figure 8.
H & E stained histological sections of rats receiving 9 doses of (A, B) 50 mg/kg and (C, D) 150 mg/kg CPT-Nva-MPs. Both show accumulation of MPs in the pulmonary capillaries (arrows). (A, C: 10X, bar and B,D: 40X).

Figure 9.
Summary of the anti-cancer efficacy results of all of the treatment groups (CPT-Nva-MPs 100 mg/kg (eq. CPT 0.22 mg/kg), CPT-Nva-MPs 50 mg/kg (eq. CPT 0.11 mg/kg), free CPT 2 mg/kg, and control (normal saline containing 0.1% Tween 80). (A) the average number (shaded bar) and average size (empty bar) of cancer sites found in lung tissue slides with complete cross section from rats receiving different treatment groups. (B) The total area occupied by cancer cells found in lung tissue slides from rats receiving different treatments. Bars represent mean±standard error of the mean (n=5).

Figure 10.
The change of body weights (BW) of animals after the inoculation of lung cancer and treatment (arrows). The increases of BW were not significantly different between groups, however, the animals receiving free CPT showed least increase of BW among all the groups.